

Electronic Supplementary Information

Highly sensitive and simultaneous detection of ctDNAs in non-small cell lung cancer serum using catalytic hairpin assembly strategy in a SERS microfluidic chip

Xiaowei Cao, *^{ace} Yu Mao,^{ace} Yuexing Gu,^{ace} Shengjie Ge,^{ace} Wenbo Lu,^b Yingyan Gu,^{ace} and Zhiyue Li^d

^aInstitute of Translational Medicine, Medical College, Yangzhou University, Yangzhou, 225001, P. R. China.

^bShanxi Normal University, College of Chemistry and Material Science, Linfen, 041004, P. R. China.

^cJiangsu Key Laboratory of Integrated Traditional Chinese and Western Medicine for Prevention and Treatment of Senile Diseases, Yangzhou University, Yangzhou, 225001, P. R. China.

^dThe First Clinical College, Dalian Medical University, Dalian, 116000, P. R. China.

^eJiangsu Key Laboratory of Experimental & Translational Noncoding RNA Research, Medical College, Yangzhou University, Yangzhou, 225001, P. R. China.

*Correspondence: cxw19861121@163.com

Result and discussion

Characterization of SERS probes

Since SERS probes were of great importance to the signal amplification, the characterization of SERS probes ($\text{Au-AgNSs@4-MBA@HP}_{1-1}$) synthesis process was performed. SERS probe was composed of three functional structures: Au-AgNSs acting as the enhancement substrate, 4-MBA acting as Raman reporter molecule, HP₁₋₁ serving as one of the CHA reactants for enhancing the SERS signal. As illustrated in Fig. S1A, a decrease was caused and the plasmon resonance at 797 nm was red-shifted to 802 nm and 814 nm respectively after the assemble of 4-MBA and HP₁₋₁ while the pure Au-AgNSs have two strong LSPR bands at about 501 nm and 797 nm. This decrease and red-shift may be caused by the slight aggregation of Au-AgNSs. To further investigate the optical properties and the stability of the prepared SERS probes, we performed an aggregation test: highly concentrated salted solution of 1 M NaCl was added to the SERS probes solution as NaCl was known to induce nanoparticle aggregation. Fig. S1B presented the UV-Vis-NIR absorption spectra of SERS probes before and after adding 1 M NaCl and it could be found that no significant changes in the LSPR spectral position and shape presented though a slight decrease appeared. Thus, BSA could efficiently chemisorbed on the Au-AgNSs surface through the strong sulfur-gold bonds, providing effective stabilization against aggregation.

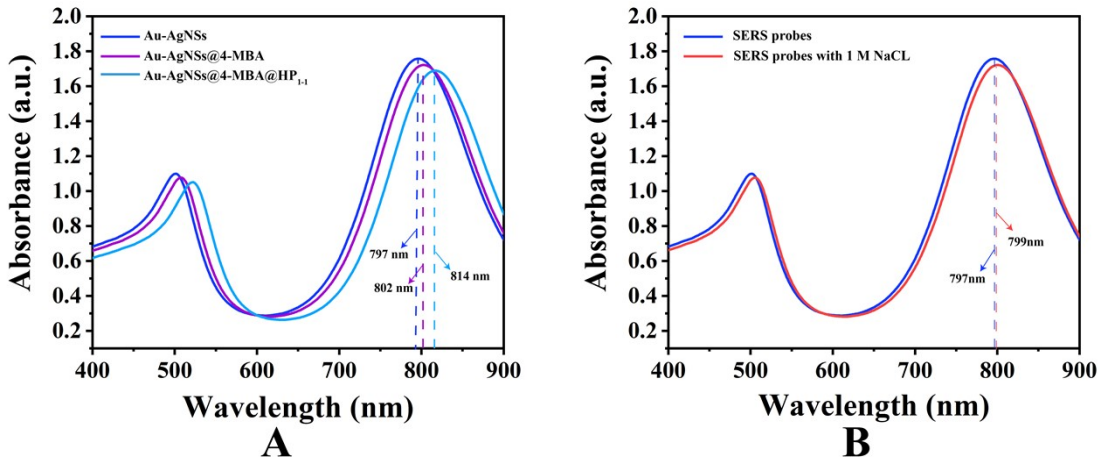


Fig. S1 Characterization of SERS probes. (A) UV-Vis-NIR spectra of Au-AgNSs, Au-AgNSs@4-MBA and Au-AgNSs@4-MBA @HP_{1.1}. (B) UV-vis spectral analysis of SERS probes after incubation in 1 M NaCl.

The Elemental mappings of Au-Ag nanoshuttles

Fig. S2 was the overlap graph of energy-dispersive X-ray (EDX) spectroscopy elemental mapping on the Au-Ag nanoshuttles. From Fig.S2, it could be found that these NSs have a homogeneous Au–Ag alloy shell around the Au NR core.

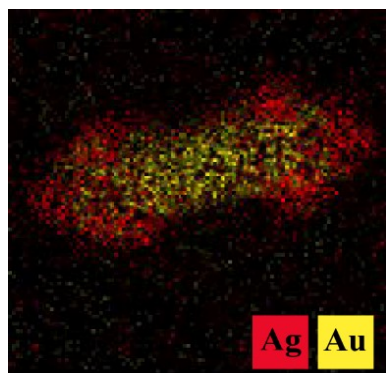


Fig. S2 Elemental mappings of Au-Ag nanoshuttles.

The hydrophilic stability of SERS microfluidic chip

The PEG-coated SERS microfluidic chip was stored at room temperature for different days (0, 1, 3, 5 and 10 d). Then the corresponding water contact angles were measured (Fig. S3). The results clearly showed highly stable hydrophilic behavior, as it only exhibited a slight increase in contact angle from 29° to 32° after 10-day storage.

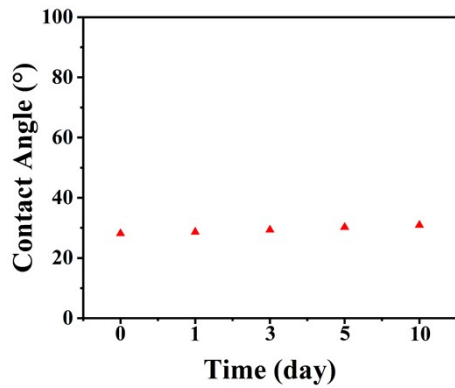


Fig. S3 Water contact angle measurements of PEG-coated SERS microfluidic chip after storing at room temperature for different days (0, 1, 3, 5 and 10 d).

Real sample application of SERS microfluidic chip

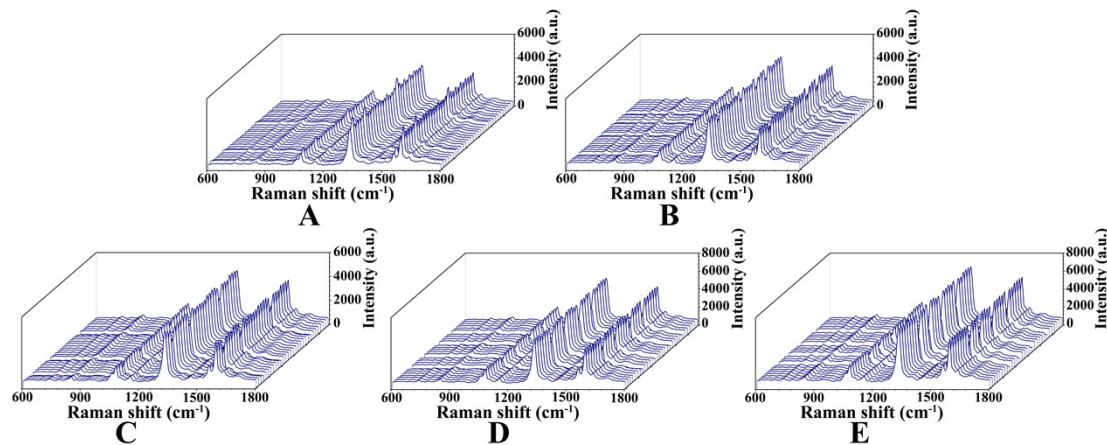


Fig. S4 Real sample application. SERS spectra of TP53 and PIK3CA-Q546K in serum obtained from healthy subjects (A) and (B) NSCLC patients at stages I, (C) II, (D) III and (E) IV.

Table S1 Comparison of the proposed microfluidic chip with other methods

Methods	Linear range	LOD	Ref.
SERS	1 fM-100 pM	9.1 fM	1
WCHA-HCR	1 fM-1 nM	3.0 fM	2
Colorimetric probe	10 fM-1 nM	20 pM	3
electrochemical	10 aM-100 nM	48 aM	4
TSDR	1 pM-100 nM	0.85 nM	5
SERS-CHA	10 aM-100 pM	2.34 aM 2.26 aM	This work

Table S2 Results of the pump-free SERS microfluidic chip and qRT-PCR for real samples (Healthy)

Sample Number	SERS (fM)		qRT-PCR (fM)		Relative error (%)	
	TP53	PIK3CA-Q546K	TP53	PIK3CA-Q546K	TP53	PIK3CA-Q546K
1	0.0202	0.0132	0.0192	0.0129	4.787	5.035
2	0.0146	0.0154	0.0141	0.0147	4.269	4.478
3	0.0200	0.0155	0.0215	0.0171	-3.685	-7.164
4	0.0214	0.0149	0.0146	0.0184	5.628	-3.711
5	0.0217	0.0187	0.0142	0.0168	3.968	6.832
6	0.0577	0.0463	0.0501	0.0454	6.561	6.449
7	0.0181	0.0197	0.0198	0.0167	-5.131	6.634
8	0.0205	0.0168	0.0185	0.0133	3.945	3.809
9	0.0161	0.0123	0.0212	0.0135	-4.235	-4.756
10	0.0210	0.0180	0.0201	0.0176	4.181	6.692
11	0.0208	0.0141	0.0176	0.0133	3.281	6.782
12	0.0186	0.0198	0.0206	0.0194	-6.472	4.312
13	0.0219	0.0175	0.0187	0.0174	3.769	5.555
14	0.0197	0.0136	0.0171	0.0129	5.933	6.567
15	0.0208	0.0164	0.0210	0.0152	-5.821	4.712
16	0.0188	0.0161	0.0178	0.0166	6.079	-4.916
17	0.0202	0.0166	0.0180	0.0159	4.145	5.639
18	0.0198	0.0157	0.0180	0.0143	4.552	5.925
19	0.0719	0.0668	0.0741	0.0662	-3.414	5.991
20	0.0191	0.0144	0.0175	0.0132	6.399	5.177
21	0.0186	0.0184	0.0182	0.0177	4.182	4.867
22	0.0167	0.0169	0.0159	0.0166	5.022	4.061
23	0.0219	0.0148	0.0172	0.0147	5.007	5.885
24	0.0593	0.0465	0.0576	0.0484	5.119	-4.545
25	0.0208	0.0201	0.0161	0.0129	4.319	5.593
26	0.0184	0.0141	0.0145	0.0124	6.304	7.053
27	0.0211	0.0157	0.0161	0.0132	5.926	4.177
28	0.0173	0.0131	0.0212	0.0189	-4.133	3.928
29	0.0177	0.0187	0.0164	0.0174	3.688	4.618
30	0.0166	0.0135	0.0158	0.0126	4.787	6.184

Table S3 Results of the pump-free SERS microfluidic chip and qRT-PCR for real samples (NSCLC I)

Sample Number	SERS (fM)		qRT-PCR (fM)		Relative error (%)	
	TP53	PIK3CA-Q546K	TP53	PIK3CA-Q546K	TP53	PIK3CA-Q546K
1	0.087	0.056	0.085	0.052	3.511	4.838
2	0.067	0.056	0.064	0.051	5.408	6.333
3	0.077	0.054	0.076	0.045	5.988	6.288
4	0.083	0.046	0.072	0.048	4.379	-5.582
5	0.084	0.059	0.063	0.043	4.592	6.221
6	0.079	0.056	0.068	0.053	3.41	5.122
7	0.012	0.020	0.016	0.022	-6.022	-5.891
8	0.078	0.048	0.073	0.049	3.507	-7.122
9	0.058	0.056	0.083	0.052	-6.174	6.394
10	0.087	0.044	0.082	0.047	3.705	-6.605
11	0.078	0.053	0.077	0.045	4.972	4.859
12	0.026	0.021	0.028	0.019	-3.987	4.679
13	0.071	0.062	0.064	0.061	4.902	6.456
14	0.073	0.056	0.057	0.051	5.377	5.993
15	0.071	0.065	0.084	0.062	-3.437	5.471
16	0.074	0.053	0.072	0.062	3.888	-7.062
17	0.084	0.058	0.082	0.051	5.381	4.791
18	0.025	0.026	0.022	0.029	5.739	-4.833
19	0.083	0.052	0.081	0.045	4.497	6.636
20	0.073	0.065	0.068	0.061	3.793	6.028
21	0.082	0.061	0.079	0.054	4.246	6.145
22	0.076	0.045	0.079	0.043	-6.475	5.681
23	0.025	0.027	0.028	0.022	-5.043	6.799
24	0.068	0.053	0.067	0.055	3.559	-5.003
25	0.064	0.046	0.061	0.043	5.549	5.322
26	0.077	0.049	0.078	0.048	-3.672	5.113
27	0.083	0.062	0.082	0.058	3.879	6.896
28	0.078	0.055	0.062	0.053	5.635	6.592
29	0.061	0.054	0.063	0.045	-5.145	5.778
30	0.074	0.042	0.079	0.062	5.726	-6.484

Table S4 Results of the pump-free SERS microfluidic chip and qRT-PCR for real samples (NSCLC II)

Sample Number	SERS (fM)		qRT-PCR (fM)		Relative error (%)	
	TP53	PIK3CA-Q546K	TP53	PIK3CA-Q546K	TP53	PIK3CA-Q546K
1	0.176	0.086	0.166	0.082	6.391	5.939
2	0.174	0.099	0.161	0.097	6.399	6.208
3	0.172	0.108	0.152	0.107	5.428	5.108
4	0.115	0.108	0.102	0.104	6.248	5.174
5	0.101	0.092	0.108	0.108	-5.956	-4.905
6	0.122	0.101	0.155	0.100	-5.609	6.845
7	0.129	0.112	0.125	0.094	6.166	4.813
8	0.183	0.097	0.148	0.098	3.362	-4.411
9	0.116	0.108	0.109	0.098	3.711	6.971
10	0.185	0.086	0.187	0.111	-3.378	-3.987
11	0.057	0.106	0.065	0.099	-5.777	5.786
12	0.187	0.103	0.165	0.106	5.761	-4.947
13	0.174	0.107	0.104	0.088	5.685	4.932
14	0.134	0.106	0.126	0.103	4.828	6.574
15	0.136	0.099	0.098	0.098	3.963	4.763
16	0.117	0.116	0.191	0.103	-4.559	3.932
17	0.139	0.109	0.108	0.108	6.286	3.679
18	0.129	0.086	0.156	0.090	-6.228	-4.538
19	0.187	0.110	0.154	0.112	4.029	6.294
20	0.117	0.094	0.172	0.091	-4.783	6.856
21	0.175	0.093	0.129	0.092	4.898	4.434
22	0.071	0.052	0.069	0.055	3.513	-4.527
23	0.143	0.108	0.106	0.106	3.682	4.136
24	0.161	0.109	0.182	0.089	-6.184	5.084
25	0.132	0.099	0.126	0.097	6.389	3.999
26	0.181	0.088	0.168	0.086	3.28	5.996
27	0.035	0.097	0.037	0.094	-5.073	3.829
28	0.151	0.105	0.142	0.086	5.045	5.787
29	0.182	0.115	0.138	0.095	6.292	4.907
30	0.181	0.114	0.154	0.084	6.391	4.839

Table S5 Results of the pump-free SERS microfluidic chip and qRT-PCR for real samples (NSCLC III)

Sample Number	SERS (fM)		qRT-PCR (fM)		Relative error (%)	
	TP53	PIK3CA-Q546K	TP53	PIK3CA-Q546K	TP53	PIK3CA-Q546K
1	0.650	0.393	0.567	0.325	3.809	4.461
2	0.612	0.392	0.548	0.353	5.232	4.899
3	0.715	0.314	0.652	0.291	5.628	5.086
4	0.593	0.329	0.664	0.419	-5.852	-4.787
5	0.051	0.040	0.530	0.035	-4.331	6.036
6	0.557	0.339	0.546	0.288	5.421	5.801
7	0.568	0.265	0.534	0.257	5.367	5.882
8	0.601	0.415	0.501	0.382	3.427	4.118
9	0.562	0.368	0.504	0.315	3.751	6.979
10	0.061	0.031	0.058	0.033	3.379	-5.652
11	0.670	0.341	0.651	0.295	3.417	5.891
12	0.686	0.419	0.654	0.269	3.407	6.525
13	0.575	0.357	0.620	0.417	-4.005	-6.644
14	0.656	0.378	0.649	0.358	6.314	4.348
15	0.687	0.381	0.681	0.393	3.256	-4.721
16	0.061	0.029	0.063	0.031	-3.971	-6.714
17	0.636	0.419	0.604	0.372	6.586	4.527
18	0.680	0.376	0.531	0.356	4.497	3.818
19	0.506	0.387	0.504	0.340	3.504	4.017
20	0.638	0.392	0.619	0.391	4.344	4.452
21	0.585	0.388	0.563	0.370	6.224	3.913
22	0.677	0.269	0.567	0.390	4.737	-4.302
23	0.682	0.418	0.582	0.333	4.424	7.173
24	0.712	0.293	0.604	0.271	5.81	3.983
25	0.563	0.462	0.552	0.409	4.86	4.092
26	0.062	0.049	0.056	0.041	6.558	7.108
27	0.657	0.282	0.522	0.267	6.023	3.789
28	0.613	0.411	0.601	0.326	4.714	5.796
29	0.665	0.321	0.606	0.314	4.566	5.473
30	0.598	0.407	0.535	0.393	3.809	5.641

Table S6 Results of the pump-free SERS microfluidic chip and qRT-PCR for real samples (NSCLC IV)

Sample Number	SERS (fM)		qRT-PCR (fM)		Relative error (%)	
	TP53	PIK3CA-Q546K	TP53	PIK3CA-Q546K	TP53	PIK3CA-Q546K
1	1.206	0.856	1.015	0.848	4.244	4.609
2	1.187	0.840	1.102	0.773	4.961	3.871
3	1.167	0.829	1.181	0.823	4.097	6.333
4	1.293	0.836	1.289	0.767	3.761	6.482
5	1.296	0.863	1.120	0.827	4.333	6.467
6	1.196	0.729	1.148	0.756	4.002	6.878
7	1.225	0.792	0.989	0.743	3.525	3.88
8	0.286	0.316	0.256	0.321	6.482	6.957
9	1.177	0.833	1.082	0.797	4.771	6.807
10	1.226	0.770	1.182	0.808	3.291	-4.164
11	1.264	0.799	1.001	0.792	4.677	5.868
12	1.277	0.809	1.155	0.737	6.498	3.685
13	1.145	0.769	1.124	0.731	5.16	4.75
14	0.224	0.348	0.242	0.346	4.717	6.988
15	1.258	0.834	1.118	0.717	4.644	6.934
16	1.189	0.745	0.997	0.741	5.397	4.462
17	1.226	0.731	1.192	0.849	5.506	-6.874
18	0.627	0.528	0.640	0.531	3.459	6.482
19	1.141	0.786	1.247	0.780	-3.601	3.873
20	1.081	0.788	0.998	0.785	4.798	6.164
21	1.237	0.814	1.212	0.744	5.998	5.344
22	1.020	0.785	1.213	0.780	-6.438	6.267
23	1.082	0.729	1.094	0.715	-3.879	3.928
24	0.302	0.243	0.317	0.252	4.751	5.689
25	1.188	0.726	1.141	0.733	6.064	-4.043
26	1.187	0.780	1.074	0.751	6.22	5.371
27	1.254	0.863	1.031	0.864	3.587	6.488
28	1.260	0.848	1.009	0.742	5.729	5.128
29	1.243	0.837	1.181	0.749	6.012	6.527
30	1.277	0.806	1.192	0.742	4.244	4.006

Reference

- 1 X. Miao, Q. Fang, X. Xiao, S. Liu, R. Wu, J. Yan, B. Nie and J. Liu, *Front. Biosci.*, 2021, **8**, 676065.
- 2 H. Chang, Y.Y. Zhang, F. Yang, C.T. Wang and H.F. Dong, *Front. Chem.*, 2018, **6**, 530
- 3 C.K. Chen, Y.C. Shiang, C.C. Huang and H.T. Chang, *Biosens. Bioelectron.*, 2011, **26**, 3464-3468.
- 4 H. Chai and P. Miao, *Chin. Chem. Lett.*, 2021, **32**, 783-786.
- 5 S. Luo, Y. Zhang, G. Huang, S. Bo, X. Ye, M. Tao, Y. Huang, B. Li, X. Jiang, Q. Wang and L. Zheng, *Sensor. Actuat. B-Chem.*, 2021, **338**, 129857.